

## Supplemental Material

### 1. Melt-quench method

Starting with the  $\beta$ -cristobalite crystalline configuration at a density of 2.2 g/cc, we melt the system by scaling atomic velocities over a time period of 30 ps until the temperature of the system reaches 4000 K. After thermalizing for 20 ps at 4000 K, we cool the system to 1900 K over 10 ps and thermalize it for 10 ps. Repeating this cooling and relaxation cycle over a time period of 120 ps, the temperature of the system is reduced to 1400 K, 950 K, 600 K, 375 K and finally to 300 K. The silica system at room temperature is amorphous, and its structure agrees very well with neutron scattering measurements.[1] To create a silica slab for shock simulations, we remove periodic boundary conditions and passivate the dangling bonds with silanols. The silanol density on the slab surface ( $4.6 \text{ nm}^{-2}$ ) is in good agreement with experiments.[2]

### 2. Validated Interatomic Potential for Silica and Water

The interatomic potentials for silica and water consist of 2-body and 3-body terms. The 2-body terms take into account steric repulsion as well as charge-charge, charge-dipole, and dipole-dipole interactions. The 3-body potential takes into account the bending of covalent bonds. Interaction between atoms in water is treated explicitly to allow chemical reactions involving dissociation of water molecules. To describe hydrolysis reactions between water and silica, we use an environment-dependent potential to combine the water and silica potentials. The functional form of the interatomic potential for both silica and water is

$$E_{\text{tot}} = \sum_{i < j} V_{ij}^{(2)}(r_{ij}) + \sum_{i < j < k} V_{ijk}^{(3)}(\vec{r}_{ij}, \vec{r}_{ik}). \quad (1)$$

The two-body term  $V_{ij}^{(2)}$  depends on the distance between atom  $i$  and  $j$  and it consists of four terms, which take into account steric repulsion, Coulomb, charge-dipole and van der Waals interactions.

$$V_{ij}^{(2)}(r) = \frac{H_{ij}}{r^{\eta_{ij}}} + \frac{Z_i Z_j}{r} e^{-r/r_{1s}} - \frac{D_{ij}}{2r^4} e^{-r/r_{4s}} - \frac{w_{ij}}{r^6}, \quad (2)$$

where  $r_{1s}$  and  $r_{4s}$  are the screening lengths for the Coulomb and charge-dipole interactions, respectively. The three-body term  $V_{ijk}^{(3)}$  has the form

$$V_{ijk}^{(3)}(\vec{r}_{ij}, \vec{r}_{ik}) = B_{ijk} \exp\left(\frac{\xi}{r_{ij} - r_0} + \frac{\xi}{r_{ik} - r_0}\right) \frac{(\cos \theta_{ijk} - \cos \theta_0)^2}{1 + C_{ijk}(\cos \theta_{ijk} - \cos \theta_0)^2} \quad (r_{ij}, r_{ik} \leq r_0), \quad (3)$$

where  $\theta_{ijk}$  is the angle between  $\vec{r}_{ij}$  and  $\vec{r}_{ik}$ . We use an environment-dependent silica-water interaction potential, which again consists of two-body and three-body terms.

The interatomic potential for silica was validated by neutron scattering data for static structure factor and  $T(r)$  ( $=r^2 g(r)$ ,  $g(r)$  is the radial distribution function).[1, 3, 4] Our molecular dynamics (MD) results for elastic moduli (Young's modulus = 66.9 GPa, Bulk modulus = 39.2 GPa, Poisson's ratio = 0.22) are in good agreement with experiments.[5] The MD result for fracture toughness,  $K_{IC} = 1 \text{ MPa}\cdot\text{m}^{1/2}$ , is within the range of experimental values ( $0.8\text{-}1.2 \text{ MPa}\cdot\text{m}^{1/2}$ ).[5] Recently we performed nanoindentation

simulations and calculated the hardness of amorphous silica to be 10.6 GPa,[6] which is close to the experimental value of 10 GPa.[7]

For water under ambient conditions, we find the O-H bond length is 0.97 Å and H-O-H bond angle is 104°. These results are in good agreement with X-ray diffraction experiments.[8] We have also examined the structural properties of super-cooled water confined in nanoporous silica. We find that the mass density distribution for water is heterogeneous, and our results for radial distribution function agree remarkably well with neutron scattering studies of low-density water (0.9 g/cc) and high-density water (1.2 g/cc). [9, 10]

Our MD simulation for water-silica interface shows that the silanol concentration lies between 4.3 and 5.4 nm<sup>-2</sup> above 300 K, which is in good agreement with experimental results.[2] The calculated hydrolysis reaction energy between water and silica lies between 0.34 and 0.70 eV, depending on the reaction sites, which falls within the range of values obtained by *ab initio* calculations.[11] Also, the MD simulation results for the lowest energy structure of the gas phase orthosilicic acid are in good agreement with *ab initio* calculations.[12] The heat of immersion of a hydrated silica slab in water is calculated to be 0.18 J/m<sup>-2</sup>, which is also in good agreement with experimental values.[13]

### 3. Modeling of gas particles

The interaction between inert gas particles is modeled by 6-12 Lennard Jones interaction with parameters for Helium. The interaction between inert gas atoms and water molecules is modeled by a steric repulsion term ( $1/r^{12}$ ), which makes the bubble insoluble and stable in water. Before the application of shock wave, the gas bubble was in equilibrium with water.

### 4. Simulation Conditions

Amorphous silica and water systems were prepared independently in the micro-canonical ensemble using periodic boundary conditions (PBC). PBC was removed in silica after thermalization and the dangling silicon and oxygen atoms on the silica surface were passivated by -OH and +H groups, respectively. Water molecules were then added around the silica slab and the system was again thermalized in the micro-canonical ensemble. Water molecules were removed from a prescribed region to create a nanobubble. In case of gas-filled bubble, the empty space was filled with inert gas atoms and the system was equilibrated in the micro-canonical ensemble.

### 5. Results

Empty bubble movie: <http://cacs.usc.edu/supplementary/BubbleCollapse/empty.mov>

This simulation movie has three parts. Part 1 shows the silica slab and the nanobubble in yellow and blue, respectively. The green and blue regions are unshocked and shocked parts in the central plane of the system. Part 2 shows the formation of a high-speed water nanojet from nanobubble collapse. The jet is represented by velocity field streamlines. Part 3 shows the formation of vortex rings when the nanojet hits the silica slab.

Gas-filled bubble movie: <http://cacs.usc.edu/supplementary/BubbleCollapse/gas.mov>

This simulation movie shows shock-induced shape deformation in a partially collapsed gas-filled nanobubble in water near the silica slab.

H<sub>3</sub>O<sup>+</sup> movie: <http://cacs.usc.edu/supplementary/BubbleCollapse/h3o.mov>

This movie shows the increase of H<sub>3</sub>O<sup>+</sup> ions in water during the collapse of a gas-filled nanobubble.

## 6. Chemical Damage in Cavitation Pit

Figure S1 shows a close up view of the center of the damaged volume. Here Si and O atoms in silica are shown in yellow and orange, respectively. Cyan and Blue spheres represent H and O atoms in water, respectively. The figure shows a large number of SiOH groups in the damaged volume.

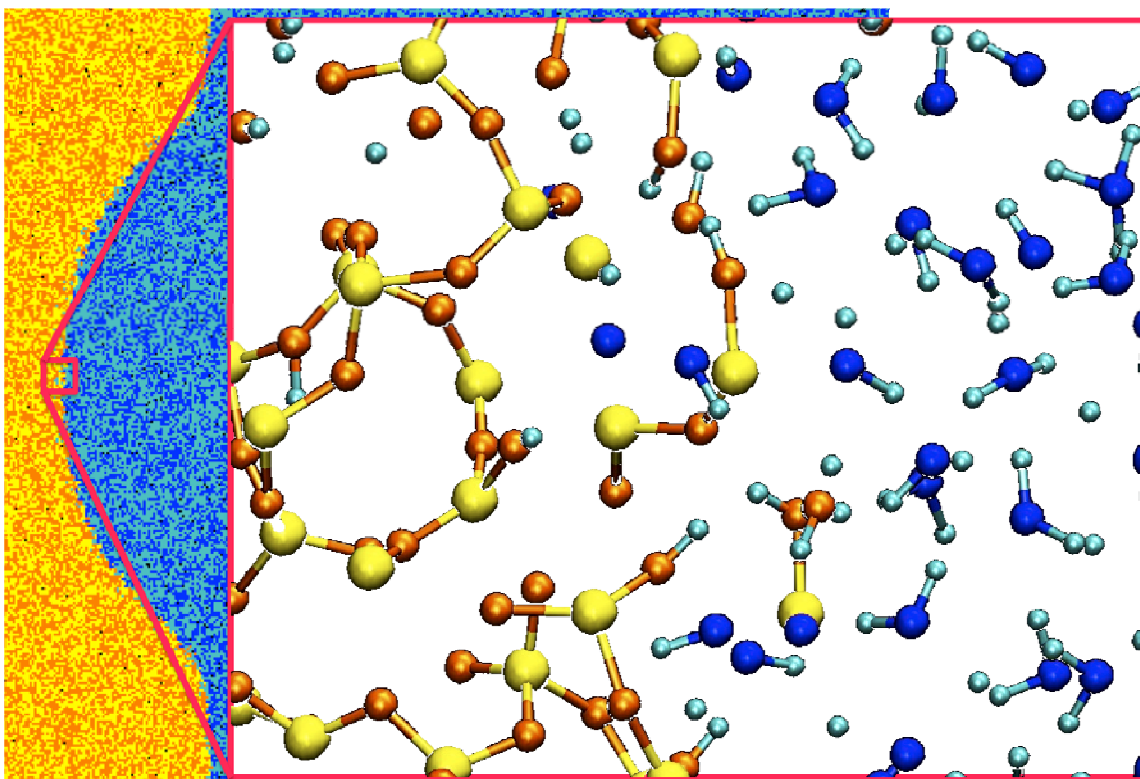


Figure S1: Close-up view of the chemical damage in the cavitation pit

## 7. References

- [1] A. C. Wright, J Non-Cryst Solids **159**, 264 (1993).
- [2] L. T. Zhuravlev, Colloids and Surfaces A: Physicochemical and Engineering Aspects **173**, 1 (2000).
- [3] P. A. V. Johnson, A. C. Wright, and R. N. Sinclair, J Non-Cryst Solids **58**, 109 (1983).
- [4] S. Susman, K. J. Volin, D. L. Price, M. Grimsditch, J. P. Rino, R. K. Kalia, P. Vashishta, G. Gwanmesia, Y. Wang, and R. C. Liebermann, Phys Rev B **43**, 1194 (1991).
- [5] Q. Wang, G. A. Saunders, H. B. Senin, and E. F. Lambson, J Non-Cryst Solids **143**, 65 (1992).
- [6] K. Nomura, Y. C. Chen, R. K. Kalia, A. Nakano, and P. Vashishta, Appl Phys Lett **99**, 111906 (2011).
- [7] K. Miyake, N. Satomi, and S. Sasaki, Appl Phys Lett **89**, 031925 (2006).

- [8] A. H. Narten, and H. A. Levy, The Journal of Chemical Physics **55**, 2263 (1971).
- [9] A. K. Soper, and M. A. Ricci, Phys Rev Lett **84**, 2881 (2000).
- [10] A. Shekhar, R. K. Kalia, A. Nakano, P. Vashishta, C. K. Alm, and A. Malthe-Sorensen, to be published (2013).
- [11] T. Bakos, S. N. Rashkeev, and S. T. Pantelides, Phys Rev Lett **88**, 055508 (2002).
- [12] J. Sauer, The Journal of Physical Chemistry **91**, 2315 (1987).
- [13] A. A. Hassanali, and S. J. Singer, The Journal of Physical Chemistry B **111**, 11181 (2007).